Where Are White Roofs More Effective in Cooling the Surface?

Linying Wang[1] , Maoyi Huang[2,3] , and Dan Li[1]

[1]Department of Earth and Environment, Boston University, Boston, MA, USA, [2]Atmospheric Sciences and Global Change Division, Pacific Northwest National Laboratory, Richland, WA, USA, [3]Now at Office of Science and Technology Integration, National Weather Service, National Oceanic and Atmospheric Administration, Silver Spring, MD, USA

Abstract By reflecting more sunlight, white (cool) roofs experience lower surface temperatures and produce less heating of the surrounding air. The effectiveness of cool roofs, quantified by the surface temperature difference between cool and regular roofs (ΔT_s), is known to vary spatially. A common perception is that ΔT_s is controlled by solar radiation that reaches the roof surface. Here we use an Earth System Model and a surface energy balance model to show that the spatial variability of ΔT_s, when normalized by the albedo difference between cool and regular roofs $\Delta\alpha$, is also controlled by an energy distribution factor that encodes the efficiencies of surface energy balance components in dissipating heat. Our results suggest that painting the roof white is more effective when the roof has less water-holding capacity and smaller thermal admittance and is located in places with more solar radiation, less precipitation, and lower wind speed.

Plain Language Summary Solar reflective roofs (also called white or cool roofs) are a common heat mitigation strategy. By increasing the albedo of roof surface, more sunlight is reflected, leading to less heating of the building and the surrounding air. In this study, the effectiveness of cool roofs is represented by the reduction of roof surface temperature per unit increase of roof albedo. Previous studies have demonstrated that this effectiveness varies spatially, but the controlling factors of the spatial variability remain unquantified. We find that the cool roof effectiveness is mainly controlled by the solar radiation that reaches the roof surface and an energy distribution factor that encodes efficiencies of different surface energy components in dissipating heat. Our results suggest that painting the roof white is more effective when the roof is located in places with more solar radiation, lower wind speed, less precipitation, and when the roof has less water-holding capacity and smaller thermal admittance. These findings shed new insights into how we implement heat mitigation strategies in urban environments. We stress that our study only focuses on the surface temperature, acknowledging that the impacts of cool roofs on air temperature and building energy consumption require further investigations.

1. Introduction

Albedo management is widely viewed as a viable option to combat extreme heat (Seneviratne et al., 2018). By increasing the albedo of land surface, more sunlight is reflected, leading to less heating of the ground and the surrounding air. In cities, roofs comprise of about 40% of the horizontal surfaces (Jackson et al., 2010) and offer a great platform for albedo management (Akbari et al., 2009; Akbari & Matthews, 2012). Widespread adoption of white roofs has already been seen in many cities such as Chicago (Mackey et al., 2012) and New York (NYC °CoolRoofs, 2012) and is becoming an increasingly important heat mitigation strategy under a warming climate and with continued urbanization (Rosenzweig et al., 2010).

To quantify the impacts of cool roofs on urban temperatures, numerical models are often employed. Most previous modeling studies focused on the reduction of near-surface air temperature at city (Broadbent et al., 2020; Fallmann et al., 2013; Georgescu et al., 2013; Li et al., 2014; Lynn et al., 2009; Salamanca et al., 2016; Schubert & Grossman-Clarke, 2013; Sharma et al., 2016; Synnefa et al., 2008; Taha et al., 1999; Vahmani et al., 2016) or neighborhood (Middel et al., 2015; Taleghani et al., 2016) scales. A common finding, as reviewed elsewhere (Krayenhoff & Voogt, 2010; Santamouris, 2014; Yang et al., 2015), is that the near-surface air temperature response to increases in roof albedo varies substantially across cities and neighborhoods. For example, Synnefa et al. (2008) used a mesoscale model (the fifth generation Pennsylvania

State University-National Centre for Atmospheric Research Mesoscale Model or MM5) to investigate the impact of roof albedo increase in Athens, Greece and found that increasing the roof albedo from 0.18 to 0.63 (0.85) could result in reduction of near-surface air temperature in the urban core as much as 1.3°C (1.6°C). However, Li et al. (2014) used the Weather Research and Forecasting (WRF) model and showed that with a similar amount of increase in the roof albedo (from 0.3 to 0.7), the near-surface air temperature reduction is about 0.5°C in the Baltimore-Washington D.C. metropolitan area, USA. By summarizing results from dozens of numerical studies in the literature, it is reported that the near-surface air temperature reduction per 0.1 roof albedo increase ranges from 0.1 to 0.33 K with a mean value of 0.2 K (Santamouris, 2014). Using a slightly different metric (near-surface air temperature reduction per 0.1 neighborhood-scale albedo increase), Krayenhoff and Voogt (2010) also found substantial variations among various case studies.

A few continental- to global-scale studies have demonstrated the spatial variability of the effectiveness of cool roofs (Akbari et al., 2012; Georgescu et al., 2014; Irvine et al., 2011; Jacobson & Ten Hoeve, 2012; Menon et al., 2010; Millstein & Menon, 2011; Oleson et al., 2010; Zhang et al., 2016). In particular, using the Community Earth System Model (CESM) with prescribed sea surface temperature, a global study found that increasing the roof albedo to 0.9 causes the largest near-surface air temperature reductions in Arabian Peninsula and Brazil where the initial roof albedo is low and the roof fraction per unit urban land is high (Oleson et al., 2010), as expected. Similar results were seen in a more recent study, which also used CESM but with a slab ocean model (Zhang et al., 2016). Oleson et al. (2010) further found that the spatial variability of near-surface air temperature response to roof albedo increase is mainly caused by changes in absorbed solar radiation and specification of roof thermal admittance, a parameter that depends on both the roof thermal conductivity and heat capacity (Oke et al., 2017). However, a theoretical framework that enables diagnosis of key controlling factors for the effectiveness of cool roofs remains lacking.

Here we provide a novel, physically based framework based on the surface energy balance to quantify the effectiveness of cool roofs, defined as the reduction of roof surface temperature per unit increase of roof albedo ($\Delta T_s / \Delta \alpha$). The effectiveness of cool roofs could also be defined based on the near-surface air temperature (Broadbent et al., 2020). We focus on the roof surface temperature, instead of near-surface air temperature, because it is the quantity that most directly responds to changes in the roof albedo. In contrast, the response of near-surface air temperature to changes in roof albedo depends on atmospheric processes in the urban canopy layer and urban roughness sublayer, which are poorly understood and parameterized in current meteorological models (Krayenhoff & Voogt, 2010). We combine the theoretical framework with global simulations generated by CESM to demonstrates that the spatial variability of $\Delta T_s / \Delta \alpha$ is controlled by the solar radiation reaching the roof surface and a surface energy distribution factor that encodes the efficiencies of roof surface energy balance components in dissipating heat.

2. Materials and Methods

The numerical experiments are conducted with the Community Land Model (CLM) Version 5 (Lawrence et al., 2019), which is the land component of the Community Earth System Model (CESM) Version 2 (Danabasoglu et al., 2020) and includes an urban model called the CLM-Urban (CLMU). The CLMU has a roof module that handles the energy and water balances over roof surfaces, which is the focus of our study. Details about the CLMU model can be found elsewhere (Danabasoglu et al., 2020; Oleson, 2012; Oleson, Bonan, Feddema, & Vertenstein, 2008; Oleson, Bonan, Feddema, Vertenstein, & Grimmond, 2008; Oleson et al., 2011; Oleson & Feddema, 2020). To simulate fractional increases in cool roofs, we improve the CLMU by separating the roof module into two parts: the regular roof and the cool roof. The regular roof albedo comes from a global data set (Jackson et al., 2010) (see Figure S1 in the supporting information), which also provides many other input parameters needed by CLMU such as roof heat capacity and thermal conductivity, while the cool roof albedo is a global constant that can be set and changed by the user. The momentum, energy, and water fluxes between the roof and the near-surface air are weighted averages of those from the regular roof and the cool roof. Here we highlight that the model always computes the temperatures and fluxes of the regular and cool roofs even when one of their fractions is set to be 0. Hence, for each experiment (regardless of the fractions of regular and cool roofs) the effectiveness of cool roofs simulated by CESM can be computed as

$$\left(\frac{\Delta T_s}{\Delta \alpha}\right)_{CESM} = \frac{T_s^{cool} - T_s^{regular}}{\alpha^{cool} - \alpha^{regular}} \tag{1}$$

where the superscripts "cool" and "regular" denote cool and regular roofs, respectively. However, when one of their fractions is 0 (say when the cool roof fraction is 0), the atmosphere simply does not receive the cool roof fluxes. In our study, all albedo values refer to the snow-free albedo values.

Based on an initial condition provided by the default CESM code (which has been spun up), we run the CLM model at 0.9° latitude by 1.25° longitude without cool roof for another 80 years by recycling the 1991–2010 Global Soil Wetness Project Phase 3 (GSWP3) atmospheric forcing (Lawrence et al., 2019) four times as further spin up. All simulations conducted in this study use the same initial condition resulting from this 80-year spin up run and the initial condition for cool roof is identical to the initial condition for regular roof. For land-only (uncoupled to an atmospheric model) simulations, we conduct 20-year runs using the same atmospheric forcing from 1991 to 2010. In the control (CTL) case, there is 0% cool roof (see Table S1). We also conduct another four 20-year sensitivity experiments (Cases 1–4, Table S1) in which we increase the fractions (50% and 100%) of cool roofs with two different albedo values (0.5 and 0.7). It should be noted that land-only simulations do not imply that the near-surface air temperature is the same in these cases with different cool roof albedo values and fractions, since the atmospheric forcing is applied at 30 m above the ground. The near-surface air temperature in these land-only simulations still respond to the increase of cool roof fraction and albedo (Figure S2). However, these land-only simulations preclude any large-scale feedbacks in the atmosphere (e.g., boundary layer, cloud, and precipitation) as well as ocean and sea ice feedbacks.

In addition to land-only simulations, a land-atmosphere coupled simulation (100% cool roof with albedo value of 0.7) is conducted. The atmospheric model used in this land-atmosphere coupled simulation is the Community Atmosphere Model (CAM) Version 6, which is the atmosphere component of CESM. The land-atmosphere coupled simulation follows the Atmospheric Model Intercomparison Project (AMIP) protocol for the historical period (Gates et al., 1999) and uses prescribed sea surface temperatures (SSTs), solar variations and aerosol chemistry from 1990 to 2010. We treat the first year as further spin up for the atmospheric model and the analysis focuses on the period 1991–2010 similar to land-only simulations.

For all simulations, we modify the CLMU code to output the daily mean surface temperatures and all fluxes, including incoming and outgoing shortwave and longwave radiation, sensible heat flux, latent heat flux, and ground heat flux, associated with regular and cool roofs. We also output the daily mean aerodynamic resistance (r_a, see Equation S2) and the evaporation efficiency (β, see Equation S3) for both regular and cool roofs, as well as the pressure, air density, and near-surface air temperature for the urban land. These daily mean outputs are used for our analysis throughout the paper. It should be pointed out that the CLMU model represents three different types of urban land: tall building district, high density, and medium density. For each grid cell, urban outputs are area averages over these three types of urban land. In this paper, we only show results for grid cells that have more than 0.1% of urban land (i.e., the sum of tall building district, high density, and medium density needs to be larger than 0.1%). In addition to daily mean model outputs, we use the static model input data such as roof albedo, roof emissivity, roof heat capacity, and roof thermal conductivity. Their area-averaged values across the three types of urban land are used to represent the average roof properties (see Figure S1 for an example about regular roof albedo).

3. Results

3.1. Reduction of Roof Surface Temperature per Unit Increase of Roof Albedo ($\Delta T_s/\Delta\alpha$)

As mentioned earlier, we perform multiple 20-year land-only and land-atmosphere coupled simulations from 1991 to 2010 at a spatial resolution of 0.9° latitude by 1.25° longitude to quantify the reduction of roof surface temperature per unit increase of roof albedo (see Table S1). Here we focus on the land-only simulations and will discuss the land-atmosphere coupled simulations later. In addition to a control (CTL) case where no cool roof is adopted, four sensitivity cases (Cases 1–4) are conducted in which we increase the fractions (50% and 100%) of cool roofs with two different albedo values (0.5 and 0.7).

We find CESM simulated $\Delta T_s/\Delta\alpha$ from these different cases to be consistent with each other (Figure S3), despite that these cases have different near-surface air temperatures (Figure S2). The majority of $\Delta T_s/\Delta\alpha$
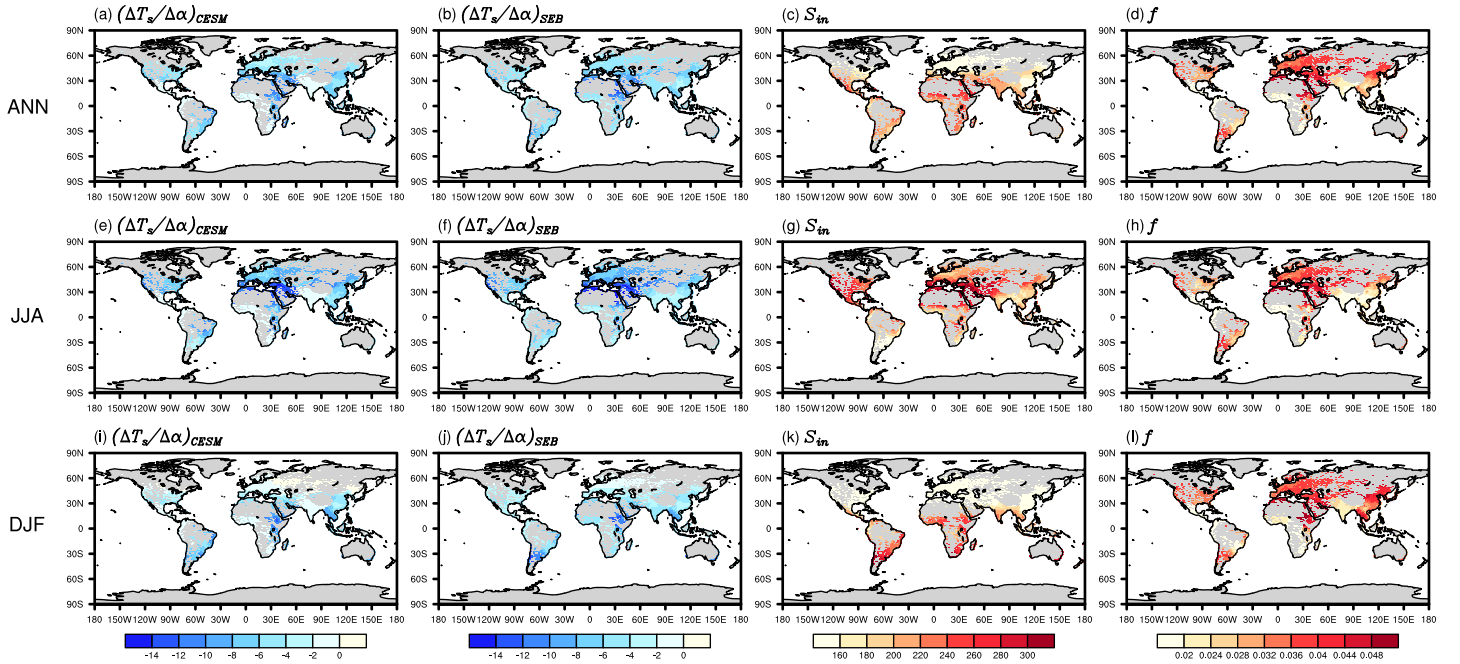
Figure 1. Roof surface temperature reduction in response to roof albedo increase (unit: K) simulated by (a) CESM and predicted by (b) SEB. Also shown are the (c) incoming solar radiation (unit: W m^{-2}) and (d) surface energy distribution factor f (unit: K W^{-1} m^2). (a–d) The annual daily mean (ANN), (e–h) the JJA daily mean, and (i–l) the DJF daily mean results over 20 years (1991–2010). The results shown here are from Case 4 (100% cool roof with albedo value of 0.7). Only grid cells with more than 0.1% of urban land are shown.

values at annual (ANN) scales and in June, July, and August (JJA) range from −8 to −4 K. In December, January, and February (DJF), the magnitude of $\Delta T_s/\Delta\alpha$ is slightly smaller with the majority ranging from −4 to 0 K. These values are broadly consistent with previous studies that examined the response of surface temperature (in addition to near-surface air temperature) to roof albedo change (Li et al., 2014; Menon et al., 2010; Yang et al., 2015).

Figure 1 shows the reduction of roof surface temperature per unit increase of roof albedo in Case 4, denoted as $(\Delta T_s/\Delta\alpha)_{CESM}$, which has a cool roof fraction of 100% and cool roof albedo of 0.7. One can see the strong spatial variability of $(\Delta T_s/\Delta\alpha)_{CESM}$. At annual scales, regions with relatively large sensitivity include the Southeast Asia, the Arabian Peninsula, the Mediterranean region, the eastern part of Africa, and Brazil. Comparing the JJA to DJF results, it is evident that the Northern Hemisphere has higher sensitivities in JJA but lower sensitivities in DJF than the Southern Hemisphere, suggesting an important role of solar radiation.

To provide a theoretical basis for understanding the CESM results, we employ a surface energy balance (SEB) model (Bateni & Entekhabi, 2012), which predicts the reduction of roof surface temperature due to roof albedo increase as (see Text S1):

$$\left(\frac{\Delta T_s}{\Delta\alpha}\right)_{SEB} = -S_{in}f \qquad (2)$$

where S_{in} is the solar radiation that reaches the roof surface and f is a surface energy distribution factor $f = \dfrac{1}{\dfrac{1}{r'_a} + \dfrac{1}{r'_o} + \dfrac{1}{r'_g} + \dfrac{1}{r'_e}}$. The $1/r'_a$, $1/r'_o$, $1/r'_g$, and $1/r'_e$ represent the efficiencies of sensible heat flux, longwave radiation, and ground heat flux (in this case the ground means the roof substrate), and latent heat flux, respectively, in dissipating heat. This model builds on but is different from a growing number of models recently used for attributing surface temperature anomalies induced by land use and land cover changes (Burakowski et al., 2018; Chen & Dirmeyer, 2016; Lee et al., 2011; Li et al., 2019; Li & Wang, 2019; Liao

Table 1
The Ranges of Pearson Correlation Coefficients Computed From CTL and Cases 1–4

Correlation coefficients	ANN	JJA	DJF
$\Delta T_s/\Delta\alpha$ and S_{in}	(−0.18, −0.17)	(−0.59, −0.56)	(−0.52, −0.51)
$\Delta T_s/\Delta\alpha$ and f	(−0.69, −0.66)	(−0.85, −0.82)	(−0.28, −0.27)
f and $1/r_a'$	(0.13, 0.14)	(0.08, 0.09)	(0.09, 0.09)
f and $1/r_o'$	(−0.16, −0.15)	(−0.07, −0.06)	(−0.25, −0.25)
f and $1/r_g'$	(−0.76, −0.75)	(−0.69, −0.68)	(−0.73, −0.72)
f and $1/r_e'$	(−0.59, −0.58)	(−0.71, −0.71)	(−0.52, −0.51)

et al., 2018; Luyssaert et al., 2014; Moon et al., 2020; Rigden & Li, 2017; Wang et al., 2019; Zhao et al., 2014) as it explicitly treats the ground heat flux (in this case the heat flux into the roof substrate) as a function of the surface temperature through the force-restore method (Dickinson, 1988). For more details including model assumptions, we refer the readers to Text S1.

The SEB model captures the spatial patterns of $(\Delta T_s/\Delta\alpha)_{CESM}$ with R^2 values of 0.60, 0.72, and 0.64 for ANN, JJA, and DJF, respectively. The differences between $(\Delta T_s/\Delta\alpha)_{CESM}$ and $(\Delta T_s/\Delta\alpha)_{SEB}$ are small (Figure S4). These differences are caused by the errors in linearizing the SEB equation and driving the SEB model with daily mean inputs and also the use of several parameterizations such as the force-restore method for the ground heat flux in the SEB model. From Equation 2 one can clearly see that the effectiveness of cool roof is determined by two factors: the insolation (S_{in}) and the surface energy distribution factor (f), both shown in Figure 1. By contrasting the patterns of $(\Delta T_s/\Delta\alpha)_{SEB}$ and S_{in}, one can appreciate the importance of f. For example, India has a comparable S_{in} as the south Asia but shows a weaker sensitivity due to a smaller f. Similar results can be seen from the comparison between the western part of Africa and the eastern part of Africa.

To quantify whether S_{in} or f controls the spatial variability of $\Delta T_s/\Delta\alpha$ more strongly, we compute the Pearson correlation coefficients between $\Delta T_s/\Delta\alpha$ simulated by CESM and S_{in} or f in all land-only simulations (i.e., CTL and Cases 1–4 in Table S1) and the ranges of correlation coefficients are shown in Table 1. All correlation coefficients shown in Table 1 have p values less than 0.001. At the annual scale and in JJA, the spatial variations in $\Delta T_s/\Delta\alpha$ are more strongly correlated with those in f (the negative sign comes from the negative sign in Equation 2). In DJF, although $\Delta T_s/\Delta\alpha$ is more strongly correlated with S_{in}, the spatial variations of f still play an important role. These results indicate that while S_{in} remains an important factor in modulating the effectiveness of cool roofs as traditionally thought, the importance of f in determining the spatial variability of $\Delta T_s/\Delta\alpha$ should be recognized.

3.2. Surface Energy Distribution Factor (f)

The surface energy distribution factor (f) encodes the efficiencies of different surface energy balance components in dissipating heat (see Text S1). Fundamentally, these efficiencies indicate how easily a heat flux can be altered by a perturbation to the surface (Bateni & Entekhabi, 2012). For example, if the efficiency for sensible heat flux ($1/r_a'$) is large, it means that the surface has a strong tendency to alter the sensible heat flux when a perturbation is applied (e.g., when albedo increases). Physically, the efficiency for sensible heat flux ($1/r_a'$) is controlled by the capability of atmospheric turbulence in transporting heat, which is a strong function of mean wind speed (Garratt, 1992). As the mean wind speed increases, the efficiency for sensible heat flux ($1/r_a'$) tends to increase, namely, it becomes easier for the sensible heat flux to respond to a perturbation to the surface. The efficiency for latent heat flux ($1/r_e'$) is controlled by the capability of atmospheric turbulence in transporting water vapor (which is assumed to be identical to $1/r_a'$) as well as the moisture availability at the surface (Brutsaert, 1982), the latter of which is often more important over dry surfaces (e.g., impervious roof surfaces). The moisture availability over roofs is controlled by the precipitation amount and the water-holding capacity (or maximum ponding depth) of roofs, as impervious surfaces only evaporate when there is ponding resulting from precipitation events (Ramamurthy & Bou-Zeid, 2014). This effect is parameterized in the CLMU (Oleson, Bonan, Feddema, & Vertenstein, 2008). The efficiency for ground heat flux ($1/r_g'$) is controlled by the thermal admittance, the importance of which in determining the capability of urban surfaces in storing heat and modulating the amplitude of urban surface temperature has long been recognized (Oke et al., 2017). The efficiency for outgoing longwave radiation ($1/r_o'$) is controlled by the near-surface air temperature (see Text S1). The reason that f (and thus the magnitude of $\Delta T_s/\Delta\alpha$) is inversely proportional to these efficiencies is because if the surface could not dissipate heat through radiation (outgoing longwave radiation), convection (sensible heat flux), conduction (ground heat flux) and/or evaporation (latent heat flux), solar radiation would heat the surface more strongly. Under such conditions, increasing the albedo, which reduces the solar energy input to the system, would be more effective in reducing the surface temperature.
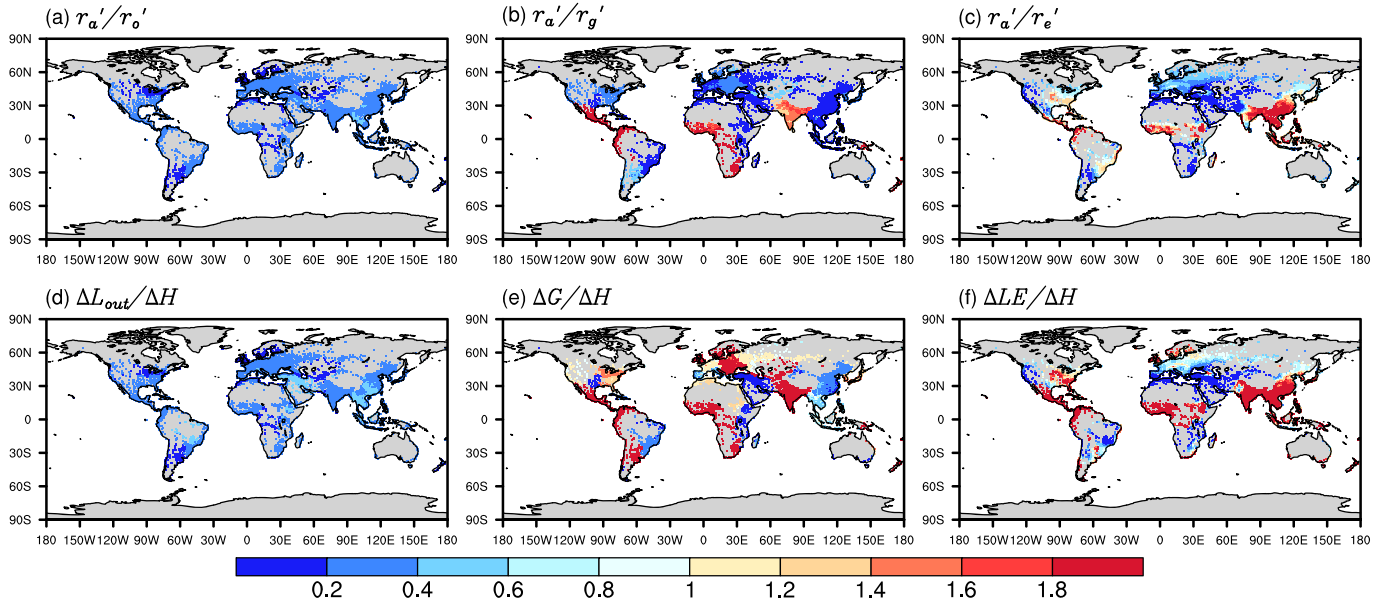
Figure 2. The ratios of efficiencies for (a) outgoing longwave radiation, (b) ground heat flux, and (c) latent heat flux to the efficiency for sensible heat flux of the roof surface, and the corresponding ratios of changes in (d) outgoing longwave radiation, (e) ground heat flux, and (f) latent heat flux to changes in sensible heat flux in response to roof albedo increase. The results are the JJA daily mean over 20 years (1991–2010) from Case 4 (100% cool roof with albedo value of 0.7). Only grid cells with more than 0.1% of urban land are shown.

To demonstrate the importance of these efficiencies, Figure 2 shows that the ratios of r_a'/r_o', r_a'/r_g', and r_a'/r_e' capture the ratios of $\Delta H/\Delta L_{out}$, $\Delta H/\Delta G$, $\Delta H/\Delta LE$ for the roof surface, respectively, in JJA where ΔH, ΔL_{out}, ΔG, and ΔLE are the changes in sensible heat fluxes, outgoing longwave radiation, ground heat fluxes, and latent heat fluxes in response to increases in roof albedo. The correlation coefficients between the resistance ratios and the flux ratios in Figure 2 are 0.98, 0.85, and 0.27, respectively. All correlation coefficients have p values less than 0.001. The lower correlation coefficient between r_a'/r_e' and $\Delta H/\Delta LE$ highlights the strong nonlinearity in the relation between latent heat flux and surface temperature (Brutsaert, 1982), which is removed in the SEB model through linearization. Similar results for ANN and DJF are shown in Figures S4 and S5. This suggests that the responses of different surface energy balance components to increases in roof albedo can be captured by these efficiencies.

Figure 3 shows the magnitude of these efficiencies for ANN, JJA, and DJF. One can see that the efficiencies for sensible heat flux ($1/r_a'$) and outgoing longwave radiation ($1/r_o'$) show much weaker spatial variability compared to the counterparts for ground heat flux ($1/r_g'$) and latent heat flux ($1/r_e'$). The efficiency for sensible heat flux ($1/r_a'$) is almost an order of magnitude larger than that for outgoing longwave radiation ($1/r_o'$), implying that when the albedo increases, the roof has a stronger tendency to reduce its sensible heat flux than its outgoing longwave radiation in order to reach a new energy balance state. This is consistent with a previous theoretical study showing that the outgoing longwave radiation is generally the least efficient mechanism over land surfaces (Bateni & Entekhabi, 2012).

The efficiencies for ground heat flux ($1/r_g'$) and latent heat flux ($1/r_e'$) are smaller than the efficiency for sensible heat flux ($1/r_a'$) for most regions but show distinct hot spots. For example, India and the western Africa have large efficiency for ground heat flux, leading to very small surface energy distribution factor (f). This explains why these regions have smaller $\Delta T_s/\Delta\alpha$ than their counterparts in similar latitudes as alluded to earlier. In the SEB model, the efficiency for ground heat flux ($1/r_g'$) is fully determined by the thermal admittance. In regions like India and the western Africa (as well as other places like the central America), the thermal admittance of the roof for both medium density and high density urban types is high due to the use of materials such as corrugated metal with little or no insulation (Jackson et al., 2010; Oleson et al., 2010; Oleson & Feddema, 2020). While our results are consistent with the input urban parameters from a global
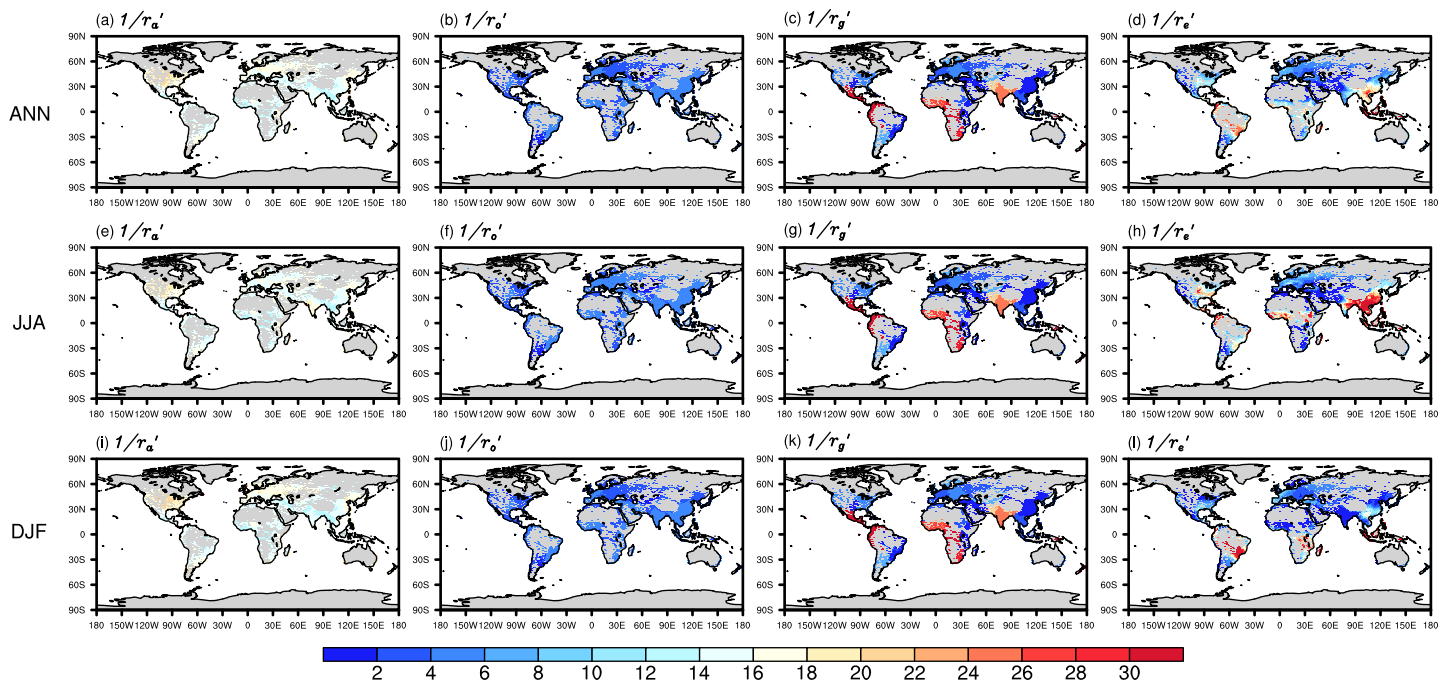
Figure 3. The efficiencies for (a) sensible heat flux, (b) outgoing longwave radiation, (c) ground heat flux, and (d) latent heat flux. All units are K^{-1} W m^{-2}. (a–d) The annual daily mean (ANN), (e–h) the JJA daily mean, and (i–l) the DJF daily mean results over 20 years (1991–2010). The results shown here are from Case 4 (100% cool roof with albedo value of 0.7). Only grid cells with more than 0.1% of urban land are shown.

data set (Jackson et al., 2010), whether these parameters faithfully reflect the true world is beyond the scope of this study. We note that there are ongoing efforts to improve these input urban parameters (Ching et al., 2018).

At first glance, it might be surprising to see that latent heat fluxes from evaporation play such an important role in many regions such as the Southeast Asia and Brazil. However, previous studies have shown that evaporation from impervious surfaces in urban environments (e.g., roofs) is a significant component of the total urban evapotranspiration (Ramamurthy & Bou-Zeid, 2014). In addition, theoretical work indicates that the efficiency for latent heat flux tends to be the largest when the surface is moist (Bateni & Entekhabi, 2012). That is, the latent heat flux tends to respond to perturbations more strongly than the other heat fluxes. Hence, the importance of evaporation for modulating the roof's surface temperature response to albedo change is expected. Given that in the CESM model roofs only evaporate when there is ponding (i.e., from precipitation events) and roofs have globally uniform water-holding capacity (= 1 mm), the spatial variability of the efficiency for latent heat flux ($1/r_e'$) is strongly controlled by the spatial variability of rainfall (Figure S7), with R^2 values of 0.69, 0.66, and 0.73 for ANN, JJA, and DJF, respectively.

Lastly, we examine the correlations between f and the four efficiencies. We find that the spatial variations of f are more strongly correlated with the efficiencies for ground heat flux and latent heat flux (Table 1), consistent with the findings in Figure 3. This does not imply that the other heat fluxes (especially sensible heat flux) are not important, but rather indicates that the efficiencies for the other heat fluxes have relatively small spatial variations (Figure 3). We highlight that although a previous study (Oleson et al., 2010) reported the importance of thermal admittance (or the efficiency for ground heat flux) in controlling the spatial variability of $\Delta T_s/\Delta\alpha$, the importance of the efficiency for latent heat flux as reported in this study is discovered for the first time.

4. Conclusion and Discussion

In this study, we address the question of where we should paint the roof white to maximize the reduction of roof surface temperature per unit increase in roof albedo ($\Delta T_s/\Delta\alpha$). Based on Earth System Model

simulations and a surface energy balance model, we find that the spatial variability of $\Delta T_s / \Delta \alpha$ is controlled by the solar radiation reaching the roof surface and a surface energy distribution factor that encodes efficiencies of different roof surface energy components in dissipating heat.

4.1. Large-Scale Feedbacks

The results presented above are from land-only simulations where the atmospheric forcing is prescribed. To examine whether allowing the atmosphere to respond to the adoption of cool roofs at the same spatial resolution would alter the results, we also perform a land-atmosphere coupled simulation (Case 5, see Table S1), with the caveat that current-generation global Earth System Models do not capture urban-scale atmospheric processes and feedbacks. As can be seen from Figure S8 and Table S2, the main findings are not changed when using the land-atmosphere coupled simulation of the same spatial resolution. This is consistent with a previous global study that compared the temperature reductions from adopting cool roofs produced by land-only simulations and land-atmosphere coupled simulations and found nearly identical spatial patterns at annual scales (Oleson et al., 2010). In addition, global modeling studies with CESM that further allow the ocean to respond found insignificant impacts of adopting cool roofs on the global mean air temperature (Zhang et al., 2016), although an earlier study using a different global model showed the possibility of warming the earth overall after adopting cool roofs due to cloud and high-latitude snow and sea ice feedbacks (Jacobson & Ten Hoeve, 2012).

4.2. The Applicability of the SEB Model

Our simulations are conducted at 0.9° latitude by 1.25° longitude spatial resolution and it is important to understand whether our findings apply to smaller scales (e.g., city or even neighborhood). While the simulation results might be dependent on the spatial resolution and model physics, the SEB model is firmly based on the surface energy balance with a key assumption that the only difference between regular and cool roofs is their albedo (see Text S1). This implicitly assumes that regular and cool roofs share the same atmospheric conditions and building interior temperature, as well as other properties such as emissivity. Therefore, when this assumption is satisfied, we expect Equation 2 to be applicable across scales. For example, in mesoscale models which are widely used to study the impacts of cool roofs at city scales, when the cool roofs are compared to the regular roofs within the same grid cell (i.e., using subgrid-scale information in a similar way as our study), they are indeed often assumed to share the same atmospheric conditions and building interior temperature (Li et al., 2014). Under such conditions, we expect that Equation 2 can be used to diagnose the simulation results from mesoscale models. On the other hand, when comparing cool roofs and regular roofs in separate simulations produced by mesoscale models, which is common in the literature (Georgescu et al., 2013; Lynn et al., 2009; Sharma et al., 2016; Synnefa et al., 2008; Taha et al., 1999; Vahmani et al., 2016), or comparing different neighborhoods using computational fluid dynamics models (Middel et al., 2015; Taleghani et al., 2016), cool roofs and regular roofs can experience different atmospheric conditions through feedbacks, which have been shown to be scale-dependent (Li & Wang, 2019), and/or different building interior temperatures. In such cases, the differences in the atmospheric conditions and building interior temperatures further contribute to the surface temperature difference between regular and cool roofs and should be taken into account.

4.3. Implications for Cool Roof Strategy

The spatial patterns shown in Figures 1 and 3 are dependent on the spatial patterns of roof parameters (e.g., thermal admittance and water-holding capacity) and atmospheric variables (e.g., incident solar radiation, precipitation, and wind speed). Acknowledging the potentially large uncertainties in these parameters and variables in global models, one shall not base the policy implications of this study for cool roof strategy on the spatial patterns shown in Figures 1 and 3, but rather the physical interpretation of Equation 2.

Equation 2 suggests that painting the roof white is more effective when the roof (a) receives more solar radiation, (b) is located in places with lower wind speed and thus weaker turbulent mixing, (c) has less water-holding capacity and receives less rainfall, and (d) has smaller thermal admittance (e.g., thicker and better insulated roof). Although the outgoing longwave radiation is more efficient in hotter places, it is generally the least efficient mechanism for land surfaces to dissipate heat (see Figure 3), and hence, its implication is not highlighted here. Condition (a) is straightforward to understand and is consistent with common perception. However, Conditions (b)–(d) are more difficult to grasp as they are rooted deeply in the heat

transfer mechanisms within the roof material and between the roof surface and the atmosphere. Together Conditions (b)–(d) imply that the solar radiation, if not reflected, would heat the roof surface much more dramatically as it is more difficult for the roof to dissipate the heat through convection, conduction, and latent heat transfer. Hence, increasing the roof albedo would be more efficient to reduce the surface temperature.

The policy implications discussed here are strictly based on the effectiveness of cool roofs being defined as the reduction of surface temperature per unit albedo increase. Adoption of cool roofs can have other impacts such as reducing building energy consumption and near-surface air temperature, which have further implications on carbon emissions, air quality, and human health (Akbari et al., 2009; Santamouris, 2014; Yang et al., 2015). While we do not quantify those impacts in this study, it is conjectured that many of those impacts are likely to be correlated with the reduction of surface temperature in summer seasons when cool roofs are expected to play the most important role. We also acknowledge that in winter seasons the reduction of surface temperature might increase building energy consumption and cause stronger atmospheric stability, which could potentially worsen the air quality (Epstein et al., 2017). These impacts are left for future investigations.

Data Availability Statement

CESM/CLM5 release code (tag: release-cesm2.0.02) is available online (http://www.cesm.ucar.edu/models/cesm2/release_download.html). The modified codes and postprocessing scripts are online (https://doi.org/10.5281/zenodo.3934414).

References

Akbari, H., & Matthews, H. D. (2012). Global cooling updates: Reflective roofs and pavements. *Energy and Buildings*, *55*, 2–6. https://doi.org/10.1016/j.enbuild.2012.02.055

Akbari, H., Matthews, H. D., & Seto, D. (2012). The long-term effect of increasing the albedo of urban areas. *Environmental Research Letters*, *7*, 024004. https://doi.org/10.1088/1748-9326/7/2/024004

Akbari, H., Menon, S., & Rosenfeld, A. (2009). Global cooling: Increasing world-wide urban albedos to offset CO_2. *Climatic Change*, *94*(3-4), 275–286. https://doi.org/10.1007/s10584-008-9515-9

Bateni, S. M., & Entekhabi, D. (2012). Relative efficiency of land surface energy balance components. *Water Resources Research*, *48*, W04510. https://doi.org/10.1029/2011WR011357

Broadbent, A. M., Krayenhoff, E. S., & Georgescu, M. (2020). Efficacy of cool roofs at reducing pedestrian-level air temperature during projected 21st century heatwaves in Atlanta, Detroit, and Phoenix (USA). *Environmental Research Letters*. https://doi.org/10.1088/1748-9326/ab6a23

Brutsaert, W. (1982). *Evaporation into the atmosphere: Theory, history, and applications*. Dordrecht, Holland: Reidel. https://doi.org/10.1007/978-94-017-1497-6

Burakowski, E., Tawfik, A., Ouimette, A., Lepine, L., Novick, K., Ollinger, S., et al. (2018). The role of surface roughness, albedo, and Bowen ratio on ecosystem energy balance in the Eastern United States. *Agricultural and Forest Meteorology*, *249*, 367–376. https://doi.org/10.1016/j.agrformet.2017.11.030

Chen, L., & Dirmeyer, P. A. (2016). Adapting observationally based metrics of biogeophysical feedbacks from land cover/land use change to climate modeling. *Environmental Research Letters*, *11*(3), 034002. https://doi.org/10.1088/1748-9326/11/3/034002

Ching, J., Mills, G., Bechtel, B., See, L., Feddema, J., Wang, X., et al. (2018). WUDAPT: An urban weather, climate, and environmental modeling infrastructure for the Anthropocene. *Bulletin of the American Meteorological Society*, *99*(9), 1907–1924. https://doi.org/10.1175/bams-d-16-0236.1

Danabasoglu, G., Lamarque, J. F., Bacmeister, J., Bailey, D. A., DuVivier, A. K., Edwards, J., et al. (2020). The Community Earth System Model version 2 (CESM2). *Journal of Advances in Modeling Earth Systems*, *12*, e2019MS001916. https://doi.org/10.1029/2019MS001916

Dickinson, R. E. (1988). The force-restore model for surface temperatures and its generalizations. *Journal of Climate*, *1*(11), 1086–1097. https://doi.org/10.1175/1520-0442(1988)001<1086:Tfmfst>2.0.Co;2

Epstein, S. A., Lee, S. M., Katzenstein, A. S., Carreras-Sospedra, M., Zhang, X., Farina, S. C., et al. (2017). Air-quality implications of widespread adoption of cool roofs on ozone and particulate matter in southern California. *Proceedings of the National Academy of Sciences of the United States of America*, *114*(34), 8991–8996. https://doi.org/10.1073/pnas.1703560114

Fallmann, J., Emeis, S., & Suppan, P. (2013). Mitigation of urban heat stress—A modelling case study for the area of Stuttgart. *Die Erde-Journal of the Geographical Society of Berlin*, *144*, 202–216. https://doi.org/10.12854/erde-144-15

Garratt, J. R. (1992). *The atmospheric boundary layer*. Cambridge, New York: Cambridge University Press.

Gates, W. L., Boyle, J. S., Covey, C., Dease, C. G., Doutriaux, C. M., Drach, R. S., et al. (1999). An overview of the results of the Atmospheric Model Intercomparison Project (AMIP I). *Bulletin of the American Meteorological Society*, *80*(1), 29–55. https://doi.org/10.1175/1520-0477(1999)080<0029:Aootro>2.0.Co;2

Georgescu, M., Morefield, P. E., Bierwagen, B. G., & Weaver, C. P. (2014). Urban adaptation can roll back warming of emerging megapolitan regions. *Proceedings of the National Academy of Sciences of the United States of America*, *111*(8), 2909–2914. https://doi.org/10.1073/pnas.1322280111

Georgescu, M., Moustaoui, M., Mahalov, A., & Dudhia, J. (2013). Summer-time climate impacts of projected megapolitan expansion in Arizona. *Nature Climate Change*, *3*, 37–41. https://doi.org/10.1038/nclimate1656

Irvine, P. J., Ridgwell, A., & Lunt, D. J. (2011). Climatic effects of surface albedo geoengineering. *Journal of Geophysical Research*, *116*, D24112. https://doi.org/10.1029/2011JD016281

Jackson, T. L., Feddema, J. J., Oleson, K. W., Bonan, G. B., & Bauer, J. T. (2010). Parameterization of urban characteristics for global climate modeling. *Annals of the Association of American Geographers*, *100*(4), 848–865. https://doi.org/10.1080/00045608.2010.497328

Jacobson, M. Z., & Ten Hoeve, J. E. (2012). Effects of urban surfaces and white roofs on global and regional climate. *Journal of Climate*, *25*(3), 1028–1044. https://doi.org/10.1175/Jcli-D-11-00032.1

Krayenhoff, E. S., & Voogt, J. A. (2010). Impacts of urban albedo increase on local air temperature at daily–annual time scales: Model results and synthesis of previous work. *Journal of Applied Meteorology and Climatology*, *49*(8), 1634–1648. https://doi.org/10.1175/2010jamc2356.1

Lawrence, D. M., Fisher, R. A., Koven, C. D., Oleson, K. W., Swenson, S. C., Bonan, G., et al. (2019). The community land model version 5: Description of new features, benchmarking, and impact of forcing uncertainty. *Journal of Advances in Modeling Earth Systems*, *11*, 4245–4287. https://doi.org/10.1029/2018MS001583

Lee, X., Goulden, M. L., Hollinger, D. Y., Barr, A., Black, T. A., Bohrer, G., et al. (2011). Observed increase in local cooling effect of deforestation at higher latitudes. *Nature*, *479*(7373), 384–387. https://doi.org/10.1038/nature10588

Li, D., Bou-Zeid, E., & Oppenheimer, M. (2014). The effectiveness of cool and green roofs as urban heat island mitigation strategies. *Environmental Research Letters*, *9*(5), 055002. https://doi.org/10.1088/1748-9326/9/5/055002

Li, D., Liao, W., Rigden, A. J., Liu, X., Wang, D., Malyshev, S., & Shevliakova, E. (2019). Urban heat island: Aerodynamics or imperviousness? *Science Advances*, *5*, eaau4299. https://doi.org/10.1126/sciadv.aau4299

Li, D., & Wang, L. (2019). Sensitivity of surface temperature to land use and land cover change-induced biophysical changes: The scale issue. *Geophysical Research Letters*, *46*, 9678–9689. https://doi.org/10.1029/2019GL084861

Liao, W., Rigden, A. J., & Li, D. (2018). Attribution of local temperature response to deforestation. *Journal of Geophysical Research: Biogeosciences*, *123*, 1572–1587. https://doi.org/10.1029/2018JG004401

Luyssaert, S., Jammet, M., Stoy, P. C., Estel, S., Pongratz, J., Ceschia, E., et al. (2014). Land management and land-cover change have impacts of similar magnitude on surface temperature. *Nature Climate Change*, *4*(5), 389–393. https://doi.org/10.1038/nclimate2196

Lynn, B. H., Carlson, T. N., Rosenzweig, C., Goldberg, R., Druyan, L., Cox, J., et al. (2009). A modification to the NOAH LSM to simulate heat mitigation strategies in the New York City metropolitan area. *Journal of Applied Meteorology and Climatology*, *48*(2), 199–216. https://doi.org/10.1175/2008jamc1774.1

Mackey, C. W., Lee, X., & Smith, R. B. (2012). Remotely sensing the cooling effects of city scale efforts to reduce urban heat island. *Building and Environment*, *49*, 348–358. https://doi.org/10.1016/j.buildenv.2011.08.004

Menon, S., Akbari, H., Mahanama, S., Sednev, I., & Levinson, R. (2010). Radiative forcing and temperature response to changes in urban albedos and associated CO_2 offsets. *Environmental Research Letters*, *5*, 014005. https://doi.org/10.1088/1748-9326/5/1/014005

Middel, A., Chhetri, N., & Quay, R. (2015). Urban forestry and cool roofs: Assessment of heat mitigation strategies in Phoenix residential neighborhoods. *Urban Forestry & Urban Greening*, *14*(1), 178–186. https://doi.org/10.1016/j.ufug.2014.09.010

Millstein, D., & Menon, S. (2011). Regional climate consequences of large-scale cool roof and photovoltaic array deployment. *Environmental Research Letters*, *6*(3), 034001. https://doi.org/10.1088/1748-9326/6/3/034001

Moon, M., Li, D., Liao, W., Rigden, A. J., & Friedl, M. A. (2020). Modification of surface energy balance during springtime: The relative importance of biophysical and meteorological changes. *Agricultural and Forest Meteorology*, *284*, 107905. https://doi.org/10.1016/j.agrformet.2020.107905

NYC °CoolRoofs (2012). Annual Review 2011 (http://www.nyc.gov/html/coolroofs/downloads/pdf/annual_report_2011.pdf, accessed on 12.24.2019)*Rep*.

Oke, T. R., Mills, G., Christen, A., & Voogt, J. A. (2017). *Urban climates*. Cambridge: Cambridge University Press. https://doi.org/10.1017/9781139016476

Oleson, K. W. (2012). Contrasts between urban and rural climate in CCSM4 CMIP5 climate change scenarios. *Journal of Climate*, *25*, 1390–1412. https://doi.org/10.1175/Jcli-D-11-00098.1

Oleson, K. W., Bonan, G. B., & Feddema, J. (2010). Effects of white roofs on urban temperature in a global climate model. *Geophysical Research Letters*, *37*, L03701. https://doi.org/10.1029/2009GL042194

Oleson, K. W., Bonan, G. B., Feddema, J., & Jackson, T. (2011). An examination of urban heat island characteristics in a global climate model. *International Journal of Climatology*, *31*(12), 1848–1865. https://doi.org/10.1002/joc.2201

Oleson, K. W., Bonan, G. B., Feddema, J., & Vertenstein, M. (2008). An urban parameterization for a global climate model. Part II: Sensitivity to input parameters and the simulated urban heat island in offline simulations. *Journal of Applied Meteorology and Climatology*, *47*(4), 1061–1076. https://doi.org/10.1175/2007jamc1598.1

Oleson, K. W., Bonan, G. B., Feddema, J., Vertenstein, M., & Grimmond, C. S. B. (2008). An urban parameterization for a global climate model. Part I: Formulation and evaluation for two cities. *Journal of Applied Meteorology and Climatology*, *47*(4), 1038–1060. https://doi.org/10.1175/2007jamc1597.1

Oleson, K. W., & Feddema, J. (2020). Parameterization and surface data improvements and new capabilities for the Community Land Model Urban (CLMU). *Journal of Advances in Modeling Earth Systems*, *12*, e2018MS001586. https://doi.org/10.1029/2018MS001586

Ramamurthy, P., & Bou-Zeid, E. (2014). Contribution of impervious surfaces to urban evaporation. *Water Resources Research*, *50*, 2889–2902. https://doi.org/10.1002/2013WR013909

Rigden, A. J., & Li, D. (2017). Attribution of surface temperature anomalies induced by land use and land cover changes. *Geophysical Research Letters*, *44*, 6814–6822. https://doi.org/10.1002/2017GL073811

Rosenzweig, C., Solecki, W., Hammer, S. A., & Mehrotra, S. (2010). Cities lead the way in climate-change action. *Nature*, *467*(7318), 909–911. https://doi.org/10.1038/467909a

Salamanca, F., Georgescu, M., Mahalov, A., Moustaoui, M., & Martilli, A. (2016). Citywide impacts of cool roof and rooftop solar photovoltaic deployment on near-surface air temperature and cooling energy demand. *Boundary-Layer Meteorology*, *161*(1), 203–221. https://doi.org/10.1007/s10546-016-0160-y

Santamouris, M. (2014). Cooling the cities—A review of reflective and green roof mitigation technologies to fight heat island and improve comfort in urban environments. *Solar Energy*, *103*, 682–703. https://doi.org/10.1016/j.solener.2012.07.003

Schubert, S., & Grossman-Clarke, S. (2013). The influence of green areas and roof albedos on air temperatures during Extreme Heat Events in Berlin, Germany. *Meteorologische Zeitschrift*, *22*(2), 131–143. https://doi.org/10.1127/0941-2948/2013/0393

Seneviratne, S. I., Phipps, S. J., Pitman, A. J., Hirsch, A. L., Davin, E. L., Donat, M. G., et al. (2018). Land radiative management as contributor to regional-scale climate adaptation and mitigation. *Nature Geoscience*, *11*(2), 88–96. https://doi.org/10.1038/s41561-017-0057-5

Sharma, A., Conry, P., Fernando, H. J. S., Hamlet, A. F., Hellmann, J. J., & Chen, F. (2016). Green and cool roofs to mitigate urban heat island effects in the Chicago metropolitan area: Evaluation with a regional climate model. *Environmental Research Letters*, *11*(6), 064004. https://doi.org/10.1088/1748-9326/11/6/064004

Synnefa, A., Dandou, A., Santamouris, M., Tombrou, M., & Soulakellis, N. (2008). On the use of cool materials as a heat island mitigation strategy. *Journal of Applied Meteorology and Climatology*, *47*(11), 2846–2856. https://doi.org/10.1175/2008jamc1830.1

Taha, H., Konopacki, S., & Gabersek, S. (1999). Impacts of large-scale surface modifications on meteorological conditions and energy use: A 10-region modeling study. *Theoretical and Applied Climatology*, *62*(3–4), 175–185. https://doi.org/10.1007/s007040050082

Taleghani, M., Sailor, D., & Ban-Weiss, G. A. (2016). Micrometeorological simulations to predict the impacts of heat mitigation strategies on pedestrian thermal comfort in a Los Angeles neighborhood. *Environmental Research Letters*, *11*(2), 024003. https://doi.org/10.1088/1748-9326/11/2/024003

Vahmani, P., Sun, F., Hall, A., & Ban-Weiss, G. (2016). Investigating the climate impacts of urbanization and the potential for cool roofs to counter future climate change in Southern California. *Environmental Research Letters*, *11*, 124027. https://doi.org/10.1088/1748-9326/11/12/124027

Wang, P., Li, D., Liao, W., Rigden, A., & Wang, W. (2019). Contrasting evaporative responses of ecosystems to heatwaves traced to the opposing roles of vapor pressure deficit and surface resistance. *Water Resources Research*, *55*, 4550–4563. https://doi.org/10.1029/2019WR024771

Yang, J. C., Wang, Z. H., & Kaloush, K. E. (2015). Environmental impacts of reflective materials: Is high albedo a 'silver bullet' for mitigating urban heat island? *Renewable & Sustainable Energy Reviews*, *47*, 830–843. https://doi.org/10.1016/j.rser.2015.03.092

Zhang, J. C., Zhang, K., Liu, J. F., & Ban-Weiss, G. (2016). Revisiting the climate impacts of cool roofs around the globe using an Earth system model. *Environmental Research Letters*, *11*, 084014. https://doi.org/10.1088/1748-9326/11/8/084014

Zhao, L., Lee, X., Smith, R. B., & Oleson, K. (2014). Strong contributions of local background climate to urban heat islands. *Nature*, *511*(7508), 216–219. https://doi.org/10.1038/nature13462